

# Spectral analysis of thermal emission from melt pool during laser material processing

P. Koruba<sup>1</sup>, M. Ćwikła<sup>1</sup>, A. Zakrzewski<sup>1</sup>, P. Jurewicz<sup>1</sup>, J. Reiner<sup>1</sup>

1. Department of Laser Technology, Automation and Production Engineering, Wrocław University of Science and Technology, Wrocław, Poland

## Abstract

This study concerns a development of simulation model for laser material processing in scope of designing an optical system for integration of confocal displacement sensor to laser head. The main issue considered was the level of radiation emitted by the melt pool during laser remelting process that affect the signal registered by the sensor. As a solution for estimating the value of radiance generated by the melt pool a simulation model build within Comsol Multiphysics software was chosen. Such a model turned out to be more accurate when comparing with experimental data from spectrometer than theoretical black or gray body simplifications with assumed values of emissivity coefficient and estimated value of melt pool temperature basing on pyrometer measurement.

## Introduction

Laser technologies such as welding, cutting and metal deposition are widely used in the industry. High quality requirements regarding process products cause that there is often a need to monitor the process [1]. For this purpose, optical sensors integrated with a laser head are often used. This allow measuring in particular the melt pool geometry as well as distance from the laser head to sample or measure keyhole depth during laser welding [2].

Within this issue we have developed an optical system that integrates the confocal displacement sensor with optical laser head [3]. The integration utilized a standard monitoring port of laser head. Therefore, the optical path of laser processing system and displacement sensor are consistent in the part of optical head. The system's principle of operation is based on longitudinal chromatic aberration. The beam generated from an external broad spectrum light source after passing through optical components of the system is directed to the material. However, considering chromatic aberration phenomenon only one wavelength will be well-focused on this material. Consequently, after reflection, this one wavelength creates a characteristic spectral peak on the system's detector which in most cases is an optical spectrum analyzer. However, the measurement beam acquired by the system's detector can be disturbed by high emitted radiation of visible and infrared radiation during the laser process.

The developed system is used to measure the distance between the laser head nozzle and the laser material processed. For this purpose the characteristic spectral peak related to perfectly focused wavelength on the material is analysis. However, this peak includes the focused wavelength, as well as lateral wavelengths. Therefore, for any distance, the different spots size as a function of wavelengths are obtained. As a consequence, a spectral peak similar to the Gaussian distribution is obtained. In case of the developed system, the spectral range of such peak is from 550 to 610 nm.

Therefore the knowledge of level of radiation in this spectral range during laser material processing is crucial for the operation of the system.

In this study the simulation model was developed to estimate how radiation from the laser process affects the readings of the

system whose optical axis is along normal to emitting surface. However, the most important issue is to calculate the level of radiation intensity as a function of wavelength. For this purpose, a spectral analysis using Comsol Multiphysics was carried out. The Surface to Surface Radiation interface was utilized to obtain information about radiation emitted from the melt pool since it enabled the calculation of radiation quantities for multiple spectral bands that can be easily compared with spectral data acquired during experimental studies.

Since, it is crucial to determine the value of emitted radiation from the melt pool in the wavelength spectrum of the peak, the radiation properties of the emitting surface should be considered vital. These properties were set based on literature data as well as by assuming grey body behavior of the melt pool.

In order to validate the developed model an experimental laser remelting process was carried out. It included a coaxial quantitative radiation measurement using high resolution spectrometer. The results of simulation and experimental studies were also compared with data calculated using gray body theory in order to check if the use of well-known theoretical approach can be competitive with simulation approach.

## Model inputs and material properties

The modelled laser remelting process can be considered as local since only the formation of melt pool and its temperature distribution influencing thermal radiation is taken into consideration. In this case the model inputs are heat source induced by laser beam, geometry of the sample as well as material and ambient properties.

The material selected for the laser surface remelting process modelling was austenitic stainless steel 316L. Since this material is widely used in laser material processing, it can serve as an example during simulation study on melt pool radiation. In Table 1 the properties of 316L steel in solid state that were needed for set up of developed model were gathered. In some cases a function of temperature (in K unit) was given. Some of them were extracted from Material Library of Comsol Multiphysics and other are taken from the literature [4,5].

**Table 1:** Thermophysical parameters of stainless steel 316L used within the model

Parameter	Value / function of temperature
solidus temperature, $T_{sol}$	1380°C
liquidus temperature, $T_{liq}$	1400°C
latent heat of fusion, $L_m$	290 J/g
thermal conductivity, $k$	$7.96 + 0.021 \cdot T - 4.71e^{-6} \cdot T^2$
Specific heat, $C_p$	$235.7 + 1.3 \cdot T - 0.002 \cdot T^2$
density, $\rho$ (solid)	$8058.7 - 0.2 \cdot T - 4.83e^{-4} \cdot T^2$
surface tension, $\gamma$	$1.71 - 4.27e^{-5} \cdot T$
dynamic viscosity, $\mu$	0.0006 kg/(m·s)
Coefficient of thermal expansion, $\alpha$	$1.50 + 3.81e^{-9} \cdot T$

## Numerical Model

In this paper, we present a simulation model of melt pool formation as a result of heating a material with high power laser beam. For this approach Heat Transfer in Solids and Fluids and Laminar Flow interfaces coupled by Non-isothermal Flow and Marangoni effect multiphysics from Heat Transfer Module and CFD Module were used. Moreover, we used Surface to Surface interface to perform multiband analysis of radiosity of the surface. Analyzed bands of 5 nm width were defined for visible range (550÷610 nm) which system being under our investigation operates in. Since, the considered problem can be regarded as axisymmetric, an appropriate 2D geometry was utilized. This led to the reduction of number of degrees of freedom and consequently shortening of the computation time. The developed model of laser remelting process consists of following components:

- Heat transfer model including laser heat source, convection, radiation and phase change phenomena
- Melt pool dynamics including and Marangoni effect
- Calculations of radiation properties for multiple spectral bands
- Calculation of free surface - external fluid Interface

The diode laser beam characterized by top-hat intensity distribution was defined as boundary heat source with 3.5 mm diameter and 0.2 mm size of transition zone. Those parameters

were obtained in measurement of laser caustic with Primes Focus Monitor.

Moreover the material properties of 316L steel regarding such as conductivity, viscosity and phase change parameters of 316L steel were implemented to the model. However, the respective interfaces for solid and fluid material were assigned to appropriate domain (Figure 1). It means that the fluid dynamics was calculated only for domain fluid whereas domain solid contain only the equations from Heat Transfer in Solids.

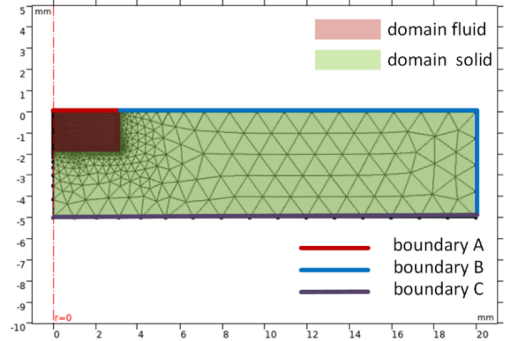


**Figure 1.** The laser remelting model with meshing and important elements marked

The model contains also a moving mesh interface (ALE approach) allowing melt pool formation (External Fluid Interface). In this case surface tension is considered as the main factor that defines geometry of the melt pool. For this reason its influence on melt pool shape will be described in detail.

## Heat Transfer model

The heat transfer phenomena (Eq. 1) included in the model contain conductivity, convection, radiation and phase change (melting and solidification). The thermal conductivity parameter was defined as a function of temperature for solid phase and a constant value for liquid phase.

$$\nabla^T (\hat{k} \nabla T) + Q_v = c_p \rho \left( \vec{u}^T \nabla T + \frac{\partial T}{\partial t} \right) \quad (1)$$

The parameters of the phase change, which are defined only for domain fluid, were presented in Table 1. In case of laser processing the shielding gas from the laser head nozzle acts as additional cooling for the substrate below. In this case, for modelling the convection heat transfer an averaged Prandtl number was calculated using the formula presented in paper [6], that described the heat transfer below the impinging gas jet. This simplification enabled to easily take into consideration the impact of shielding gas on the laser processed surface.

Advanced radiation properties implemented in the model are widely discussed in further paragraph. However, this approach concerns only surface A (Figure 2), whereas in case of other surfaces a simplifying assumption of constant value of emissivity coefficient was used with Surface to Ambient interface (boundary B). For boundary C a condition of thermal insulation was used.

Furthermore, the phase change phenomenon was added into the model for inclusion of latent heat of fusion in the heat balance. The use of liquid phase fraction gave also an opportunity to determine which part of the modelled material should be subjected to CFD equations describing melt pool dynamics.

## Melt pool dynamics model

In order to model the melt pool dynamics a Laminar Flow interface was selected. It is worth underlining that the parameters of the fluid such as dynamic viscosity ( $\mu$ ) and density ( $\rho$ ) were set as a function of temperature. Moreover, the Buoyancy (Eq. 2) force as well as Marangoni effect (Eq. 3) were implemented in domain liquid to calculate the movements of the liquid metal in the melt pool more accurately.

$$\vec{F}_B = -\rho_{liq} \vec{g} \beta_T (T - T_{ref}) \quad (2)$$

$$\mu \left( \frac{\partial u}{\partial y} \right) = - \left( \frac{\partial \sigma}{\partial T} \right) \left( \frac{\partial T}{\partial x} \right) \quad (3)$$

The surface tension forces were also considered in phenomenon of shaping the free surface of external boundary between the liquid metal and ambient. This surface may behave differently depending on the sign of surface tension coefficient which is a value assigned to the specific material. On the one hand, the topic of surface tension coefficient for stainless steel 316L is widely discussed in many papers [5]. However, the results shown in these papers indicates a great diversity in case of this particular parameter. For this purpose, a short study on resultative melt pool shapes was made in Comsol Multiphysics using different values of surface tension coefficient (Figure 2). For proper model set-up of the laser remelting model, the simulation results of melt pool size were compared with experimentally prepared samples. It allowed selecting adequate value of surface tension coefficient (Table 1).

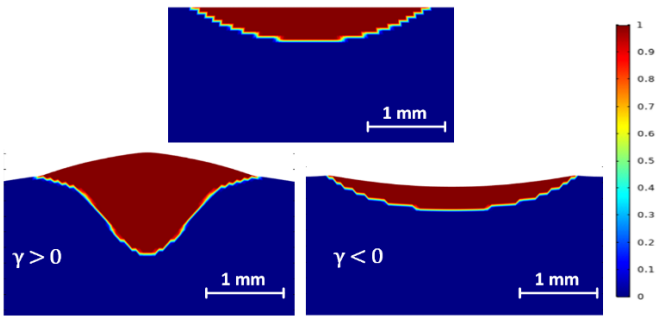


**Figure 3.** The comparison of melt pool shape in case of: no consideration of surface tension (a), positive value of surface tension coefficient (b), negative value of surface tension coefficient (c)

## Multiple spectral bands radiation model

The Stefan-Boltzmann law (Eq. 4) allows to calculate total radiation emitted by the surface for whole spectrum, but for this specific application it was necessary to analyze fraction of total emitted radiation only in spectral band defined for system. For this purpose a functionality of Multiple spectral bands in the Radiation interface was selected. It permits to divide analyzed spectrum from 500 to 650 nm with 5 nm step to see how emitted radiation vary over this range.

$$q_r = \varepsilon \sigma T^4 \quad (4)$$

The calculations were conducted with respect to two different approaches. Firstly, the emitting surface was defined as diffuse and behaves as gray body. In this case the simplification were that an average emissivity is characterized by directional

and spectral independency. In the second approach, the diffuse surface assumption remained but the emissivity was implemented as a function of wavelength. In both cases the assumption made in accordance to Kirchhoff's Law (Eq. 5) was made that absorptivity and emissivity are equal in the analyzed spectrum.

$$\varepsilon(\lambda, T) = A(\lambda, T) \quad (5)$$

The emissivity in the second approach was defined for every band separately and varied with accordance to [7], whereas in the first case was assumed constant and had been estimated using pyrometer data.

It is vital in case of system's operation that only radiation emitted from the small area of the melt pool will affect system's reading. Therefore, the area representing the melt pool was divided into smaller segments whose lengths correspond to adequate spectral bands (Figure 4). Finally, resultative emitted radiation in specific spectral bands were averaged over corresponding curves (areas) defined by spot sizes of focused on the material wavelength as well as lateral wavelengths.

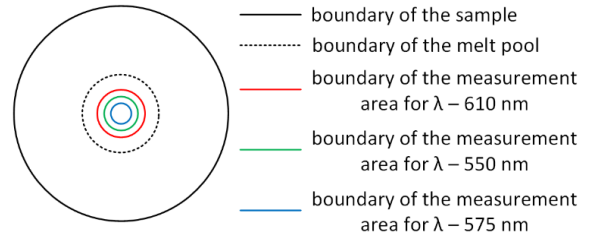


**Figure 4.** The schematics of radiosity calculation within different spectral bands taking into consideration the area of measurement by the system

## Meshing and study settings

The meshing types chosen for this study were Mapped and Free triangular for domain liquid and solid respectively. For domain liquid a very fine meshing was used in order to obtain precise results in case of fluid dynamics. The maximum element size was 0.05 mm, whereas in case of domain solid a predefined size (Normal for General Physics) was selected.

The selected type of study was time dependent and additionally a parameter sweep was used during estimation of absorptivity and emissivity coefficient assuming gray body approximation. The time of simulation was set to 3.5 seconds with time step of 0.1 second and the solution tolerance remained as physics controlled.

## Experimental Set-up

The experimental validation of developed model was divided into two parts regarding experiments carried out using black body calibrator and radiation measurements during laser remelting (Figure 5). Previously, the spectrometer was calibrated to measure the absolute unit of radiation – irradiance. The procedure of calibration consisted of measurements with high resolution spectrometer HR 4000 (Ocean Optics) and dedicated light source – lamp LS1-Cal. The measurements with black body calibrator BB-4A (Omega) enabled the comparison of irradiance measured by spectrometer with radiosity values

calculated within simulation model for constant temperature. This value was also set in black body calibrator.

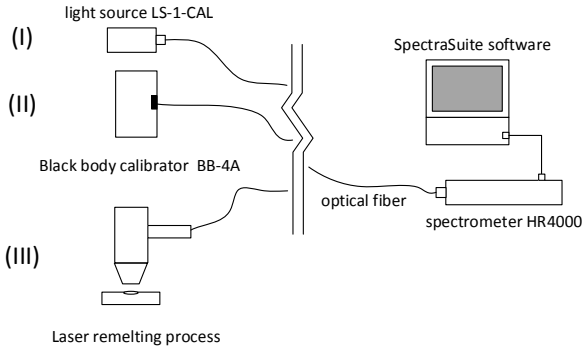


**Figure 5.** The schematics of experimental setup for simulation validation: spectrometer calibration (I), verification with black body calibrator (II), validation with laser remelting process (III)

The last part of experiment was carried out during laser remelting process. The laser system consisted of high power diode laser LDF 4000-30 (Laserline) coupled with laser optical fiber. The face of the fiber was coupled to adapter of laser optical head placed on arm of the robot RSV60-40 (Reis). The optical head including collimating lens, dichroic mirror and focusing lenses. The dichroic mirror allow to monitoring the process by analysis of decoupling radiation during laser material processing. The decoupled radiation is directed to monitoring port extensions. All of the processes were carried on using shielding gas (argon) with low volumetric flow, resulting in good protective atmosphere.

## Results and discussion

Firstly, the simulation model was simplified to describe blackbody emissive characteristics and constant temperature on the surface was assumed. The defined value of temperature in the model corresponded with value set in black body calibrator. Subsequently, numerically obtained results of radiosity were compared to theoretical calculations and results of experimental measurements of blackbody calibrator irradiation. The theoretical values of radiance were calculated using Radiance Calculator [8]. Figure 6 shows a good compliance of theoretical, simulation and experimental data for black body temperature equals 982 °C.

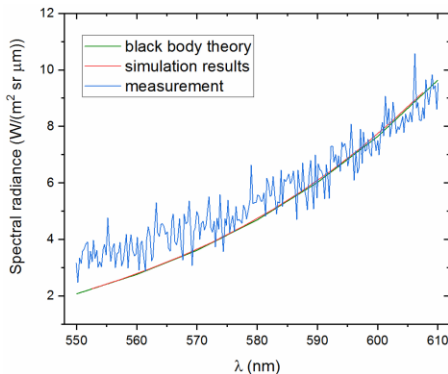


**Figure 6.** The comparison between black body theory, simulation and measurement results. In case of simulation a simplified model with constant temperature equal to the one set on blackbody calibrator

Subsequently, the radiation from the melt pool during laser remelting process was modelled and analyzed. To compare the simulation results a theoretical data of gray body radiation were utilized. However, in order to calculate the theoretical values of radiance the knowledge of the value of melt pool temperature is needed. This lead to the use of pyrometer for estimation of process temperature. The assumption of gray body behavior by the melt pool was verified by comparison of simulation and experiment. This approach can be considered as tuning the simulation to receive the same level of temperature in semi-steady state [9] The simulation of laser remelting process was calculated for different values of absorptivity and emissivity coefficients that were set equal (gray body assumption). The temperature plots extracted from simulation as well as acquired by pyrometer measurement are shown on Figure 5. By comparing the temperature values obtained both in simulation parameter sweep and measurement with pyrometer, the selected value for absorptivity and emissivity coefficients was established as 0.8.

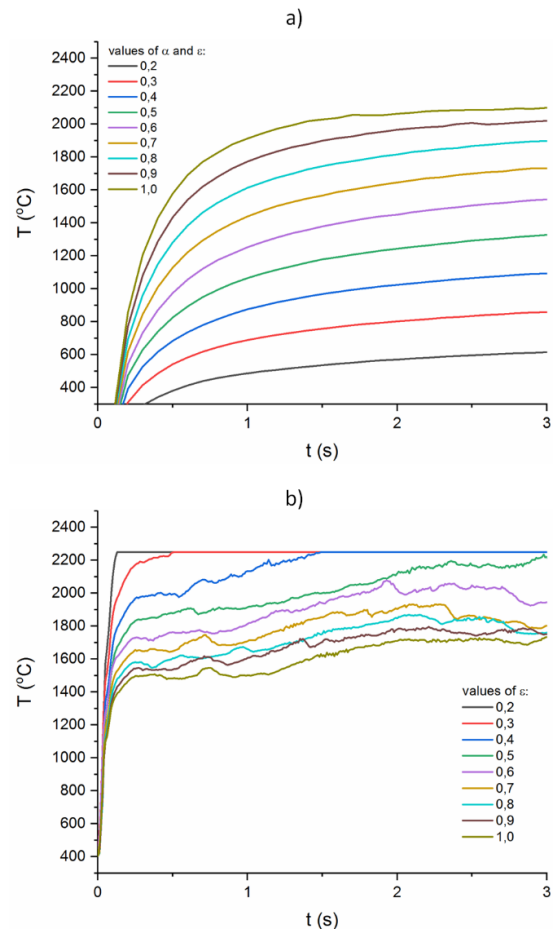


**Figure 5.** The comparison of gray body approximation (assumption of constant and equal value of absorptivity and emissivity coefficients): results of simulation tests (a), results of experimental tests with one-color pyrometer (b)

After choosing appropriate value for  $\epsilon$  and  $A$  for the second approach of simulation study, the model was calculated for both gray body assumption and literature data. Regarding the literature emissivity data two cases were analyzed i.e. for oxidized surface of 316L steel in 1200K and polished surface in 800K [7]. This make in total 3 approaches to setting the radiation properties in developed model (Figure 6).

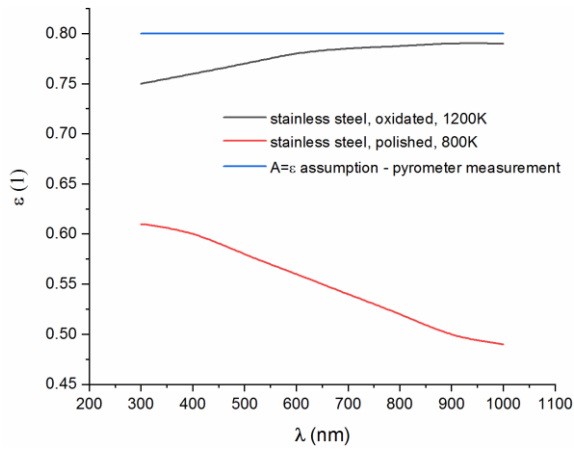


**Figure 6.** The utilized emissivity values for simulation studies

The resultative quantities calculated within the model are temperature, phase change indicators and radiosity for every considered spectral band. The results obtained in simulation with use of absorption and emissivity coefficients for oxidized surface are shown on Figure 6. From single calculated simulation one can receive the size of melt pool, its average and maximum temperature as well as time-dependent radiosity and temperature distributions.

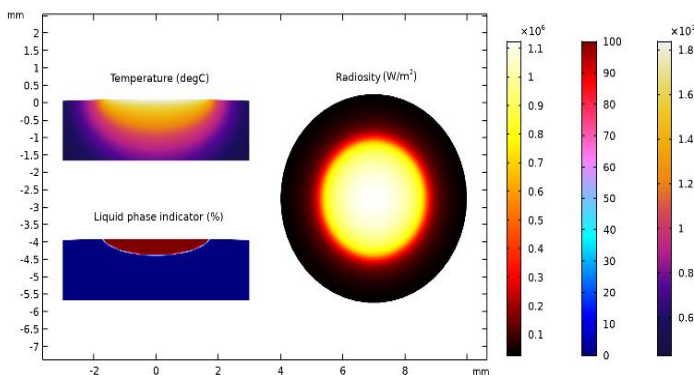


**Figure 6.** The simulation results of laser melting process including temperature distribution, liquid phase indicator and surface radiosity

Figure 7 shows a comparison of radiosity values calculated using developed model, acquired using spectrometer and using theoretical data obtained assuming gray body behavior of the melt pool ( $\epsilon = 0.8$ ). The temperatures set for gray body assumption cases was the temperature measured with the pyrometer (1930 °C) that can be associated with averaged temperature of the melt pool [10]. The second value of temperature used in gray body theoretical calculation was the maximal temperature registered in the simulation model of the melt pool (2600 °C). Furthermore, this figure contains simulation results set up as it was discussed above and experimental data acquired with the spectrometer.

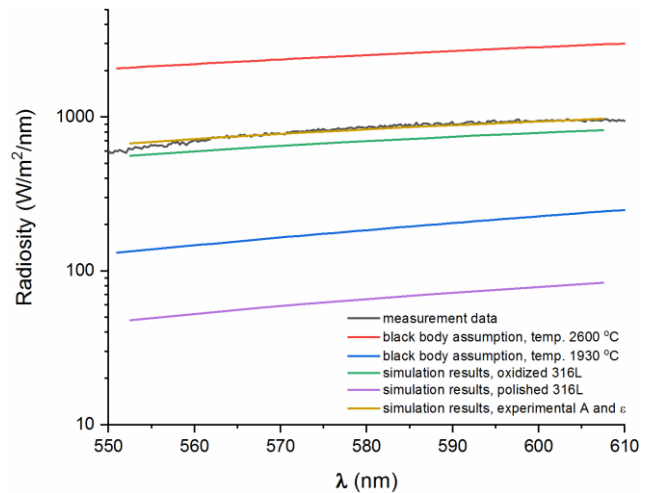


**Figure 7.** The resultative radiosities of the melt pool as a function of wavelength in visible spectrum

Comparison of theoretical, simulation and experimental results leads to conclusion that the best compliance is achieved between measurement and simulation data for gray body assumption based on radiation parameters estimation using pyrometer. Moreover, the simulation based on data for oxidized surface in 1200 K gives also quite good results when comparing to other simulation and theoretical data. It is worth underlining that using gray body or even black body theoretical calculations may lead to a significant error in estimation of level of melt pool radiation. Also an incorrect setting of absorption and emissivity values within the simulation model may result in

## Conclusions

The developed laser remelting model with spectral information about melt pool radiation serves as a good basis for design of the optical system. The comparison of simulation and experimental studies shows that combining the measurement with pyrometer with parameter sweep within developed simulation model gives the most adequate values of absorption and emissivity parameters. This kind of simulation tuning ensures better compliance with measurement that basing on literature data. Moreover, the use of theoretical data based on gray body theory cause much greater inconsistency with measurement data. This approach also requires knowledge of temperature value of the melt pool that may be the source of further errors. Summing up, using a simple black body calculator even when the approximated values of process temperature and emissivity are known leads to a significant error.

Finally, it can be concluded that simulation studies of laser remelting process with extended multispectral analysis is a good tool for approximation of the melt pool radiation affecting the signal registered by system and the developed model can be used for variety of laser processed materials.

## References

1. Hu D., Kovacevic R., Sensing, modeling and control for laser-based additive manufacturing, *International Journal of Machine Tools & Manufacture* Vol. 43, pp. 51-60 (2003).

2. Authier N., Baptiste A., Touvrey C., Bruyere V. and Namy P., Implementation of an interferometric sensor for measuring the depth of a capillary laser welding, Proceedings of the ICALEO Conference 2016, paper #904.
3. Ćwikła M., Zakrzewski A., Koruba P., Jurewicz P., Reiner J., Preliminary design of longitudinal chromatic aberration sensor implemented to laser processing head, Optics and Measurement International Conference 2019, 8-10 October 2019, Liberec, Czech Republic / Jana Kovačičinová ed. Bellingham, Wash. : SPIE, cop. 2019. art. 1138502.
4. Pichler P., Simonds B. J., Sowards J. W., Pottlacher Measurements of thermophysical properties of solid and liquid NIST SRM 316L stainless steel, Journal of Material Science, Vol 55, 4081-2093 (2020).
5. Li Z., Mukai K., Zeze M, Mills K. C., Determination of the surface tensin of liquid stainless steel, Journal of Materials Science, Vol. 40, 2191-2195 (2005).
6. Martin H., Heat and Mass Transfer between Impinging Gas Jets and Solid Surfaces, Advances in Heat Transfer, Vol.13, pp. 1-60 (1977).
7. Incropera F. P., DeWitt D. P., Bergman T. L., Lavine A. S., Fundamentals of Heat and Mass Transfer, John Wiley & Sons, Inc., Jefferson 2011.
8. Radiance Calculator <https://astrogeology.usgs.gov/tools/thermal-radiance-calculator/> (September 2020)
9. Koruba P., Radkiewicz P., Jurewicz P., Reiner J., Supervision of temperature during laser metal deposition process on aluminum alloy based on thermal simulation model, International Conference Thermography and Thermometry in Infrared 2019, Ustron, Poland.
10. De Baere D., Devesse W., Spectroscopic monitoring and melt pool temperature estimation during the laser metal deposition process, Journal od Laser Applications, Vol. 28, 022303 (2016).

## Acknowledgements

This paper was supported by The National Centre for Research and Development, project No. LIDER/18/0071/L-9/17/NCBR/2018 “Process control of laser material processing using the phenomenon of chromatic aberration”.